ACS OMEGA

http://pubs.acs.org/journal/acsodf

Article

Validation and Evaluation of High-Resolution Orbitrap Mass Spectrometry on Molecular Characterization of Dissolved Organic Matter

Qiong Pan, Xiaocun Zhuo, Chen He,* Yahe Zhang, and Quan Shi*

Cite This: *ACS Omega* 2020, 5, 5372−5379

Read Online

ACCESS | Metrics & More | Article Recommendations | Supporting Information

ABSTRACT: Molecular composition of dissolved organic matter (DOM) is a hot topic in subjects such as environmental science and geochemistry. Fourier transform ion cyclotron resonance mass spectrometry (FT-ICR MS) has been applied to molecular composition characterization of DOM successfully. However, high instrument and maintenance costs have constrained its wider application. A high-resolution Orbitrap mass spectrometer (Orbitrap MS) can provide approximately 500,000 resolving power (at m/z 200), which is potentially capable of characterizing the molecular composition of DOM. In this paper, the application of high-resolution Orbitrap MS was evaluated by comparing with FT-ICR MS in the aspect of resolution, mass distribution, detection dynamic range, and isotopic peak intensity ratio. The impact of instrument parameters of Orbitrap MS was further investigated, which includes ionization, ion transfer, and mass detection. The result shows that the high-resolution Orbitrap MS is capable or even preferable for molecular characterization of DOM. However, the peak intensity distributions are dependent on the instrument parameters, which could affect the environmental impact assessment caused by the sample itself. The result indicates that development of a universal and comparable method is of great demand.

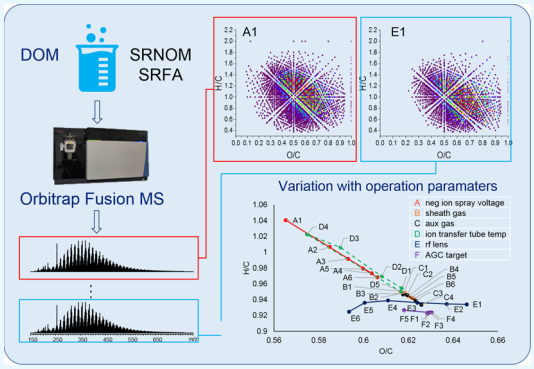

INTRODUCTION

Dissolved organic matter (DOM) is an organic mixture that usually exists in water, soil, and other environmental systems.[1−3] DOM is an important component of the global carbon cycle and plays a critical role in the global climate change.[4−7] In recent years, many scientific issues relating to DOM have become attractive topics under the situation of global climate change.[8−10] Generally, DOM is mainly composed of C, H, O, and N with minor contributions from S and P. The molecular composition of DOM is extremely complex and usually contains a number of hydroxyl, carboxyl, and other functional groups.[11] Traditional analytical methods such as infrared spectroscopy and elemental analysis only reveal information of DOM on a macroscopic property level.[12,13] The most effective method for the molecular composition analysis of DOM is mass spectrometry (MS).[14] Conventional mass spectrometry, however, has a low resolution and cannot fully characterize the DOM on the molecular level. Mass spectrometers that reach the requirements need a resolving power of more than 100,000 (at m/z 400). Fourier transform ion resonance mass spectrometry (FT-ICR MS) is an ideal method for analyzing the molecular composition of DOM.[15]

Electrospray ionization (ESI) coupled with FT-ICR MS has been applied for characterizing the DOM since the late 1990s.[16−20] Though various ionization methods, such as atmospheric pressure chemical ionization, laser desorption ionization, and paper-based spray ionization have been used in characterizing DOM, negative mode ESI has been widely accepted and preferred in the DOM research field.[2,7,8,21−35] Although FT-ICR MS provides unparalleled high resolution, the high costs of instrument, maintenance, and operation have constrained its wide application.[36,37] The Orbitrap mass spectrometer (Orbitrap MS) is a new type of commercially available high-resolution mass spectrometer. Unlike the FT-ICR MS utilizing liquid helium to maintain the superconducting magnetic field, it uses an electrostatic axially harmonic orbital trap as the mass detector.[38] The maintenance cost is much cheaper as compared to FT-ICR MS.[39,40] Since 2005 when the Orbitrap MS became commercially available, many powerful techniques have been gradually applied to Orbitrap MS, and the resolution has increased from about 150,000 to more than 450,000 (at m/z 200) in the past

Received: December 22, 2019
Accepted: February 20, 2020
Published: March 9, 2020

https://dx.doi.org/10.1021/acsomega.9b04411
ACS Omega 2020, 5, 5372−5379

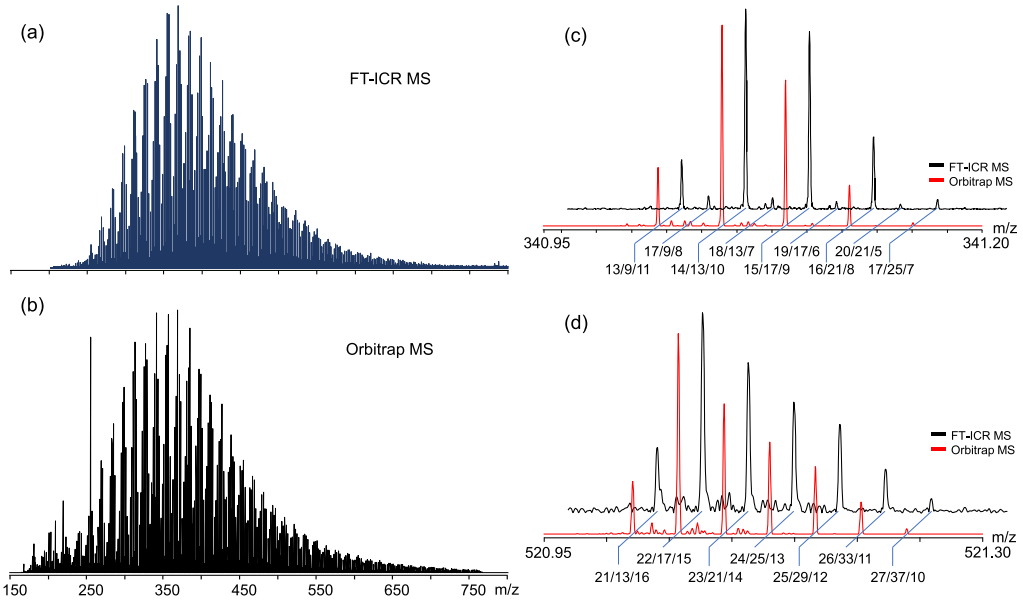

Figure 1. ESI SRNOM broadband spectra of (a) FT-ICR MS and (b) Orbitrap MS. Expanded spectra segments of FT-ICR MS (black) and Orbitrap MS (red) at (c) m/z 341 Da and (d) m/z 521 Da. C, H, and O atom numbers of peaks labeled (e.g., 17/9/8 means $[C_{17}H_{10}O_8 - H]^-$).

years.[37,38,41] Orbitrap MS showed superior ability in characterizing low-molecular-weight (MW) molecules and has been used to characterize DOM from various resources.[42−44] Additionally, the high scan rate makes the Orbitrap MS capable of coupling liquid-phase chromatography to separate and characterize DOM online.[45]

Reproducibility of MS has been a challenge in the analytical chemistry field for decades.[46−49] For Orbitrap MS, as an alternative to high-resolution MS, technology iteration and upgradation is quick. However, there is still lack of systematic evaluation of Orbitrap MS on DOM characterization, although evaluation of early models of Orbitrap Elite MS for DOM characterization has already been studied.[36,50] The resolving power, ion transmission, and versatile MS^n capability of Orbitrap MS have been improved dramatically, which calls for the demand for the evaluation of the Orbitrap Fusion MS for DOM characterization. Instrument operation is a non-negligible problem and affects the results dramatically.[51] Therefore, the extent of impact caused by instrument parameters to the environmental sample analysis should be investigated.

This paper will evaluate the applicability of the Orbitrap Fusion MS for the molecular characterization of DOM by comparing with FT-ICR MS in the aspect of resolution, mass distribution, detection dynamic range, and isotopic peak intensity ratio. The instrument parameters of ionization, ion transfer, and mass detection of the Orbitrap Fusion MS will be investigated.

RESULTS AND DISCUSSION

Validation of Orbitrap MS by Comparing with FT-ICR MS. *Molecular Weight and Peak Intensity Distribution.* Figure 1 shows the broadband and expanded spectra of FT-ICR MS and Orbitrap MS. FT-ICR MS mass spectra exhibited a maximum around m/z 350 and a mass range of m/z 200−800 (Figure 1a). The overall similar mass distribution of the Orbitrap MS mass spectra compared to that of FT-ICR MS is notable, despite that Orbitrap MS mass spectra exhibited a maximum around m/z 340 and a mass range of m/z 150−800 (Figure 1b). This is expected because of the ubiquitous discrimination of low m/z ions in FT-ICR MS.[52] This mass distribution discrimination phenomenon can be clearly demonstrated from our recent work on characterization of a crude oil. A comparison between the mass spectra of crude oil collected via the Orbitrap MS and FT-ICR MS clearly demonstrates the advantage of Orbitrap MS on low-mass molecule characterization (Figure S1 in the Supporting Information). Although negative mode ESI has been widely accepted, the profile of mass spectrum both in the mass range and peak relative abundance was affected by the ionization source and the instrument operating parameters.[46] Most of the accepted DOM spectra are composed of a series of peaks ranging from m/z 150 to 800. The peak intensity distribution of the detected masses is bell-shaped as highly degraded natural DOM shares similar molecular structures.[53]

In the expanded spectra, the peak intensity distribution at m/z 341 (Figure 1c) and m/z 521(Figure 1d) shows peaks at an odd nominal mass. The peak intensity distribution at a nominal mass is continuous. Both the number and relative intensity of peaks in these ranges obtained by the two mass spectrometers are very similar. It should be noted that the FT-ICR mass spectrometer was not running at its highest mass resolution status in order to obtain high quality peak shape and stable mass range distribution.

Mass Resolution. In Figure 1c,d, the expanded spectra of Suwannee River natural organic matter (SRNOM) at m/z 341 and m/z 521 clearly shows the predominant [CHO] compounds in the DOM, with a difference of 36.4 mDa induced by the substitution between O and CH_4. In Figure 1c, the low abundant peak series, $[C_{17}H_9O_8]^-$, $[C_{18}H_{13}O_7]^-$, and $[C_{19}H_{17}O_6]^-$, and the high abundant peak series, $[C_{13}H_9O_{11}]^-$, $[C_{14}H_{13}O_{10}]^-$, and $[C_{15}H_{17}O_9]^-$ are seen. The observation of these two series of compounds with different saturations are consistent with previous research.[33] Resolution of $[C_{14}H_{13}O_{10}]^-$ is 310,000 and 360,000 ($R = m/\Delta m_{50\%}$) in FT-ICR MS and Orbitrap MS, respectively. Kim et al.[54] studied the resolution requirements for determining the elemental composition of petroleum crude oil. At present,

https://dx.doi.org/10.1021/acsomega.9b04411
ACS Omega 2020, 5, 5372−5379

Table 1. Isotope Abundance of Mass Peaks Detected at m/z 341 (%)

			FT-ICR MS		Orbitrap MS	
molecular formula $[M-H]^-$	MW (Da)	theoretical isotopic ratio (%)	relative intensity[a] (%)	measured isotopic ratio (%)	relative intensity[a] (%)	measured isotopic ratio (%)
$C_{13}H_9O_{11}$	341.013938	14.58	22	12.50	29	8.86
$C_{14}H_{13}O_{10}$	341.050323	15.67	87	15.09	100	11.68
$C_{15}H_{17}O_9$	341.086709	16.76	78	14.01	72	12.04
$C_{16}H_{21}O_8$	341.123094	17.85	32	16.75	20	13.73
$C_{17}H_{25}O_7$	341.156480	18.94	4	25.15	2	1.41

[a]Relative intensity to the base peak in the broadband spectrum.

Table 2. Representative Indexes and Number of Detected O_{10} Class Compounds under Different Instrument Parameters[a]

				weight averaged									
ID	all[b]	O_{10}[c]	AI_{mod}	DBE	HU	H/C	O/C	C	H	O	N[d]	S[d]	MW
A1	5706	201	0.36	9.62	0.77	1.04	0.57	17.91	17.61	9.96	0.25	0.25	393.20
A2	5966	195	0.38	10.02	0.75	1.01	0.58	18.09	17.16	10.40	0.27	0.21	401.93
A3	6137	198	0.38	10.19	0.73	0.99	0.59	18.14	16.94	10.57	0.27	0.20	404.98
A4	5980	193	0.39	10.34	0.71	0.97	0.60	18.12	16.58	10.73	0.28	0.20	406.88
A5	6174	200	0.39	10.34	0.72	0.98	0.60	18.21	16.78	10.73	0.28	0.20	408.16
A6	5934	194	0.39	10.41	0.70	0.97	0.61	18.15	16.50	10.80	0.28	0.20	408.17
B1	5462	186	0.41	10.32	0.67	0.95	0.62	17.69	15.78	10.68	0.27	0.25	400.34
B2	5536	187	0.41	10.37	0.67	0.95	0.62	17.77	15.83	10.76	0.27	0.21	402.45
B3	5642	186	0.41	10.54	0.67	0.95	0.62	18.05	16.05	10.92	0.28	0.20	408.58
B4	5626	185	0.41	10.52	0.67	0.94	0.62	17.97	15.92	10.91	0.28	0.21	407.20
B5	5506	186	0.41	10.47	0.66	0.94	0.62	17.85	15.79	10.86	0.28	0.21	404.95
B6	5419	183	0.41	10.40	0.66	0.94	0.62	17.70	15.63	10.78	0.28	0.22	401.83
C1	5657	186	0.41	10.53	0.67	0.95	0.62	18.03	16.03	10.91	0.28	0.20	408.18
C2	5646	185	0.41	10.55	0.67	0.95	0.62	18.04	16.01	10.94	0.28	0.20	408.80
C3	5561	182	0.41	10.58	0.66	0.94	0.62	17.98	15.82	10.97	0.28	0.21	408.24
C4	5540	178	0.41	10.61	0.65	0.93	0.63	17.96	15.72	11.00	0.28	0.21	408.46
D1	5338	184	0.40	10.24	0.67	0.95	0.62	17.61	15.77	10.61	0.27	0.23	398.16
D2	5580	187	0.39	10.25	0.70	0.97	0.61	17.88	16.28	10.64	0.26	0.21	402.28
D3	5974	202	0.38	9.90	0.73	1.01	0.59	17.83	16.89	10.31	0.25	0.21	396.95
D4	5815	204	0.37	9.66	0.74	1.02	0.57	17.68	17.08	9.98	0.26	0.25	390.31
D5	5593	184	0.40	10.41	0.67	0.95	0.62	17.86	15.93	10.79	0.27	0.22	404.07
E1	4350	167	0.42	9.58	0.61	0.93	0.65	16.07	14.00	10.03	0.27	0.27	368.69
E2	4690	174	0.42	9.92	0.63	0.93	0.64	16.71	14.61	10.35	0.28	0.25	382.03
E3	5446	182	0.41	10.52	0.65	0.94	0.62	17.83	15.66	10.89	0.28	0.22	405.14
E4	6130	192	0.41	10.98	0.67	0.94	0.61	18.72	16.51	11.26	0.28	0.19	422.50
E5	6840	206	0.41	11.50	0.67	0.94	0.60	19.60	17.25	11.64	0.28	0.17	439.93
E6	7029	211	0.42	12.01	0.65	0.92	0.59	20.34	17.70	11.97	0.28	0.19	454.48
F1	5564	181	0.42	11.02	0.64	0.92	0.63	18.52	16.02	11.38	0.27	0.20	421.57
F2	5551	177	0.42	10.91	0.64	0.92	0.63	18.33	15.86	11.27	0.28	0.21	417.26
F3	5425	178	0.42	10.79	0.64	0.92	0.63	18.13	15.70	11.16	0.28	0.21	413.02
F4	5415	179	0.42	10.69	0.64	0.92	0.63	17.95	15.54	11.06	0.28	0.22	409.07
F5	5974	188	0.42	11.06	0.65	0.93	0.62	18.66	16.22	11.34	0.28	0.22	422.76

[a]MW, molecular weight (Da); AI_{mod}, modified aromatic index; DBE, double-bond equivalent; HU, highly unsaturated, all values are weight-averaged. [b]Total number of assigned mass peaks. [c]Number of mass peaks assigned as $CcHhO_{10}$ class compounds. [d]The value is 10 times of the original value.

FT-ICR mass spectrometers with different magnetic field strengths are configured for DOM analysis; instruments with a resolving power above 300,000 can basically meet the threshold of DOM molecular composition characterization.[54−56] Therefore, Orbitrap MS can theoretically meet the DOM analysis requirements from the perspective of resolution. It should be pointed out that the FT-ICR MS spectrum in Figure 1c is the result of averaging 64 time-domain acquisitions. Benefitting from the long signal acquisition time, the FT-ICR mass spectrometer performs better than Orbitrap MS in the detection of low-abundance compounds such as $[C_{17}H_9O_8]^-$, as shown in Figure 1c .

At high m/z values, for example, at m/z 521 Da (Figure 1d), Orbitrap MS shows good baseline. This is mainly caused by the root-cut process in data acquisition, which limits the potential custom processing on the free induction decay signal, like short-time FT.[57] The problem can be resolved by using third-party data acquisition systems, such as FTMS Booster (Spectroswiss, Switzerland).

Isotopic Peak. Table 1 shows the five kinds of compounds from m/z 341.95 to 341.20. Theoretical isotopic peak intensity

https://dx.doi.org/10.1021/acsomega.9b04411
ACS Omega 2020, 5, 5372−5379

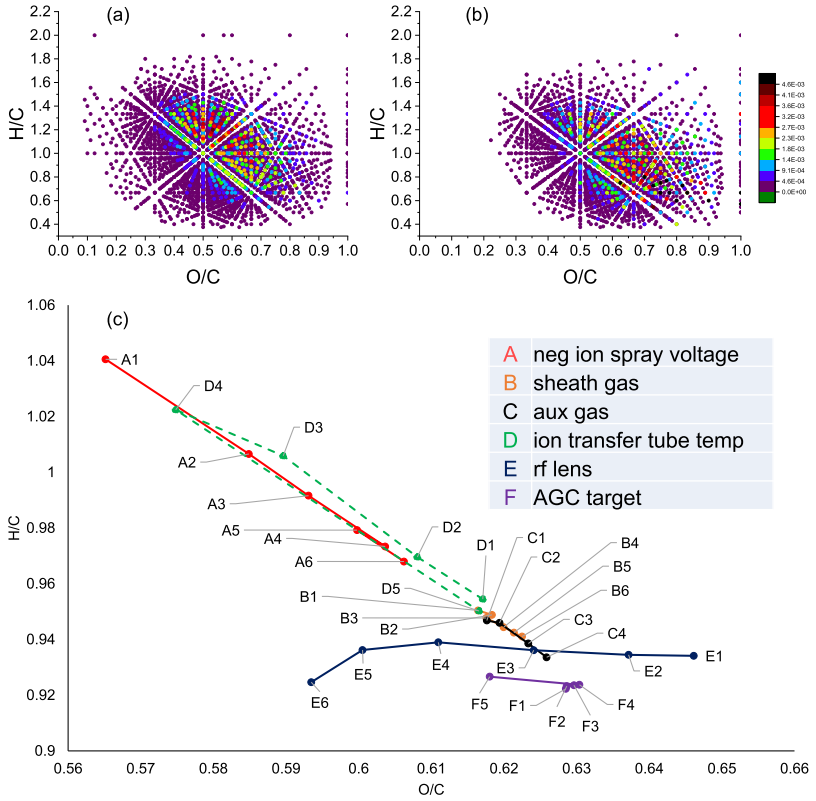

Figure 2. Van Krevelen diagram of CHO compounds in (a) A1 and (b) E1, color mapped to the normalized intensity. (c) Weight-averaged H/C and O/C values of all detected compounds under different instrument parameters.

could be calculated using IsotopePattern (Bruker) based on the natural isotope abundance of each element. The ratio of theoretical isotopic peak intensity to the monoisotopic peak intensity varies from 14 to 19%. The measured isotopic ratio of FT-ICR MS ranges from 12 to 25%, of which the formula $[C_{17}H_{25}O_7]^-$ has the biggest difference; this is because the relative intensity of the monoisotopic peak is only 4% of the base peak in the broadband spectra, and so the low intensity is of great influence on the measured isotopic ratio. The measured isotopic ratio of the other four peaks correlate well with the theoretical value (Table 1). For Orbitrap MS, all measured isotopic ratios are lower than the theoretical values, and this is caused by the root-cut of baseline as discussed above. Certainly, the lower cumulative time of Orbitrap MS affects the ion detection of low-abundance ions.

In high-resolution DOM mass spectrum, the ^{13}C isotope peak usually appears beside the N_1O_x compound peak at an even nominal mass, for example, an 8 mDa mass difference is observed between $[^{13}CC_{13}H_{13}O_{10}]^-$ and $[C_{13}H_{12}N_1O_{10}]^-$ because of the substitution between ^{13}CH and N. The presence and relative abundance of isotope peaks are of great importance in molecular formula identification; so far, many molecular formula programs have adopted isotope detection as a validation procedure.[58,59] However, Table 1 indicates that molecular formula assignment programs appropriate for FT-ICR MS may not be suitable for Orbitrap MS. Isotope abundance of Orbitrap MS is usually underestimated.

Impact of Instrument Parameters of Orbitrap MS. Suwannee River fulvic acid (SRFA) standard sample has been used widely in the DOM study; it was selected in the experiment to evaluate the impact of the instrument setting including ionization source, ion transfer optics, and mass detector on the spectrum.[23,49,60−62] The detailed parameter setting is described in the Experimental Section.

In this study, molecular information is presented by means of statistical analysis. The proportional relationship between elements such as C, H, O, S, and N is the basic parameter in representing the degree of DOM degradation. In addition, AI_{mod} is a widely used degradation index calculated through a specific computational formula.[63,64] Characteristics of each broadband spectra were revealed by accumulating relative intensities of the respective molecular formulae, which had been used in many publications.[8] Therefore, the perturbation of instrument parameters to the signal response could provide reference for the DOM study.

Neg Ion Spray Voltage. Table 2 shows the amount of O_{10} class compounds and some representative indexes commonly used for the analysis of DOM detected under each set of instrument parameters. Although the influence of ion spray voltage (group A) on the amount of detected O_{10} class compounds is slight, when the ion spray voltage increases from A1 (2600 V) to A6 (3100 V), the relative abundance of compounds with a high oxygen content, such as $[C_{14}H_7O_{11}]^-$, gradually increases. The relative abundance of compounds with a low oxygen content, such as $[C_{19}H_{27}O_6]^-$, gradually decreases (Figures S2 and S3 in the Supporting Information). Double-bond equivalent (DBE), MW, and O/C increase along with increased ion spray voltage. One possible cause is that ESI ionization sources tend to ionize polar compounds, whereas compounds with higher oxygen content have higher polarity and are more easily ionized, which lead to higher signal intensity.

https://dx.doi.org/10.1021/acsomega.9b04411
ACS Omega 2020, 5, 5372−5379

Ion Transfer Tube Temperature. As shown in Table 2, the number of O_{10} compounds detected at different ion transfer tube temperatures (group D, from 200 to 300 °C with a 25 °C gradient) increased first and then decreased as the temperature increases, and the main compounds that changed were those with more carbon atoms (Figure S4). The heat of ion transfer tube is mainly used to volatilize the solvent for better ion generation. Therefore, it is possible to explain that when the temperature is lower than 275 °C, incomplete volatilization of the solvent induced loss of these ions. However, when the temperature is higher than 275 °C, the ions are prone to chemical changes at high temperatures, resulting in a decrease in the number of detected ions. However, the change of MW and C atomic number is not obvious. The change of DBE is consistent with that of O/C, which proves that the bias of ion transfer tube temperature on DOM analysis should not be ignored.

rf-Lens. As shown in Table 2, the impact of rf-lens (group E) on the number of detected O_{10} class compounds cannot be ignored. The rf-lens is an ion transmission device consisting of progressively spaced, stainless-steel electrodes. The mass spectrometer applies an rf voltage to the electrodes; adjacent electrodes have voltages of the opposite phase. As the rf amplitude increases, ions of progressively higher mass-to-charge ratios pass through to the exit lens and move toward the subsequent optics. Along with the increasing rf-lens (group E, from 20 to 120% with a 20% gradient), the number of detected O_{10} class compounds gradually increases. When the rf-lens was 20% (E1), the m/z range of detected O_{10} class compounds was 270−545, and when the rf-lens was 120% (E6), the m/z range of detected O_{10} class compounds was 272−569. In addition, the DBE distribution range of detected O_{10} class compounds at 20% rf-lens is narrower than that at 100% (Figure S5 in the Supporting Information).

AGC Target. The number of ions injected into the detector cell is of great importance to ion detection; a small number of ions could not generate a detectable signal. As can be seen in Table 2, with the increase of the Automatic Gain Control (AGC) target (group F), the detected amount of O_{10} compounds did not change significantly. The change of other representative parameters is not obvious, which proves that the AGC target is independent of the selectivity of ions as long as the signal is stable. AGC controls the number of injected ions, regardless of ion characteristics. However, space charge interactions would reduce the dynamic range and transient lifetime once the ions became too dense. Ion injection of Orbitrap MS is determined by the instrument parameter, specific lens of AGC unit turn on or off, to control the number of ions injected. Soule et al.[46] studied the effect of AGC target on LTQ FT-ICR MS and proved that AGC target was not linearly correlated with the number of detected peaks.

Van Krevelen diagram, which takes the O/C ratio as the horizontal coordinate and H/C as the vertical coordinate, is widely used to display the compound type distribution of DOM and reveal the biochemical conversion of DOM molecules.[8,11,65] Figure 2 shows the Van Krevelen diagrams of the CHO compound under instrument parameters A1 and E1. It can be seen that more compounds with a low O/C ratio are detected under instrument parameter A1 (Figure 2a) than E1 (Figure 2b). The center of the compound distribution under A1 is around O/C = 0.55 and H/C = 1.2, whereas under E1, the center is around O/C = 0.65 and H/C = 0.9. The compound type could be classified into lipid, tannin, and other types by their region in the Van Krevelen diagram by referring to a typical compound type classification (Figure S6). It is clear that with the instrument parameter of E1, compounds which are likely to be tannin and aromatics have higher responses. Figure 2c is a derived Van Krevelen diagram, in which the relative intensities of the respective molecular formula detected under different instrument parameters were accumulated. It can be seen from Figure 2c that the ion spray voltage, ion transfer tube temperature, and rf-lens have a great influence on O/C and H/C. While comparing the data of environmental DOM samples, it can be found that not only the characteristics of the samples themselves but also the influence of the instrument parameters would affect the results. Mass spectra are impacted by multiple parameters together, and it is more complicated while evaluating all parameter combinations, although the actual instrument parameter settings vary from instrument to instrument. The purpose of this paper is not to provide parameter paradigms but to reveal the impact of instrument parameter setting on the DOM analysis.

Application Prospect of Orbitrap MS. As a new mass spectrometer, Orbitrap MS has been improved obviously in the spectrum quality for DOM analysis. Although the resolution of the instrument could not reach that of FT-ICR MS, the resolving power of Orbitrap MS can meet the requirements of DOM analysis. Moreover, an analytical method such as liquid chromatography coupled with high-resolution MS is strongly needed for a complex mixture analysis, which broadens the dimension of molecular composition information. Compared to FT-ICR MS, Orbitrap MS has a broader application prospect because of its higher scan rate as well as its detection of low MW ions (as low as 50 Da). It is obvious that as a particularly convenient and readily deployable mass spectrometer, Orbitrap MS should be considered as an alternative tool in characterizing DOM molecular composition. In some occasions, it could provide supplementary information missed in FT-ICR MS. Considering the lower instrument and maintenance costs, the prospect of Orbitrap MS for DOM characterization is optimistic.

CONCLUSIONS

Orbitrap MS is a rapidly developing technology for high-resolution MS analysis of a complex mixture. Comparing with FT-ICR MS, the Orbitrap MS has a comparable mass resolution power, an acceptable isotope ratio, a more reasonable mass distribution in the lower mass end, and a more rapid signal acquisition. Orbitrap MS is suitable for the molecular characterization of DOM in various aquatic systems and has optimistic application prospect in multiple academic communities. Instrument parameters of ionization, ion transfer optics, and mass detector have great influence on the results of the analysis. A standard method should be developed for molecular characterization of DOM as well as other complex mixtures.

EXPERIMENTAL SECTION

Samples and Reagents. SRFA and SRNOM samples were purchased from the International Humic Substances Society. Analytical grade methanol was purchased from Sinopharm Chemical Reagent, which was purified by distillation before use. SRFA and SRNOM were diluted in methanol to a final concentration of 50 μg/mL in methanol for MS analysis.

https://dx.doi.org/10.1021/acsomega.9b04411
ACS Omega 2020, 5, 5372−5379

MS Analysis. An Orbitrap Fusion MS (Thermo Scientific, USA) and a 9.4T Apex FT-ICR mass spectrometer (Bruker, Germany) were used for the molecular composition analysis of DOM. Samples were infused directly into the negative mode ESI sources at a speed of 180 μL/h. The mass range for FT-ICR MS was m/z 200−800; detailed instrumental setting for FT-ICR MS is described elsewhere.[51] For Orbitrap MS, the ranges were m/z 150−800 for SRNOM and 100−800 for SRFA. The instrument resolution mode was selected as 500,000. The sampling duration was 2 min for each acquisition, and the microscan was set at 3.[37,55,58] In the instrument parameter evaluation section, instrument parameters such as ion spray voltage, sheath gas, aux gas, ion transfer tube temperature, rf-lens, modified AGC target, and spectrums under different parameters were acquired. Detailed instrument parameters are shown in Table S1 (see the Supporting Information).

Data Analysis. Mass lists of Orbitrap MS were internally calibrated with a high-abundance homologous series and extracted using Xcalibur Qual Browser (Thermo Scientific). After averaging all scans in the collected 2 min spectrum, noise peaks with relative intensity below 0.1% were discarded. Internal calibration and extraction of mass lists of FT-ICR mass spectra were performed with DataAnalysis 3.4 (Bruker). Mass peaks with s/n magnitude greater than 6 were exported to peak lists. Molecular formula assignments of mass lists of both Orbitrap MS and FT-ICR MS were performed using custom software. The typical element constrains ($C_cH_hN_nO_oS_s$, c < 50, h < 80, o < 30, n < 4, s < 2)[23] and heuristic rules were integrated to eliminate cases where multiple formulae were assigned to the same m/z.[66,67] Also, it should be noted that all molecular formulae in this article refer to $[M - H]^-$. Relative intensities were calculated by dividing the intensity of each peak by the sum of the intensities of all assigned molecular formulae in one broadband mass spectrum.

■ ASSOCIATED CONTENT

Supporting Information

The Supporting Information is available free of charge at https://pubs.acs.org/doi/10.1021/acsomega.9b04411.

> Instrument parameters of ESI-Orbitrap MS, mass distribution of condensate oil spectra of FT-ICR MS and Orbitrap MS, distribution of O_{10} compounds under different ion spray voltages, expanded spectra under evaluated ion spray voltage at m/z 351, distribution of O_{10} compounds under 275 °C and 300 °C ion transfer tube temperatures, distribution of O_{10} compounds under 20% and 100% rf-lens, and typical category of compounds in the different areas of van Krevelen diagram (PDF)

■ AUTHOR INFORMATION

Corresponding Authors

Chen He − *State Key Laboratory of Heavy Oil Processing, Petroleum Molecular Engineering Center (PMEC), China University of Petroleum, Beijing 102249, China*; Phone: +86 10 89733738; Email: hechen@cup.edu.cn

Quan Shi − *State Key Laboratory of Heavy Oil Processing, Petroleum Molecular Engineering Center (PMEC), China University of Petroleum, Beijing 102249, China*; orcid.org/0000-0002-1363-1237; Phone: +86 10 89739157; Email: sq@cup.edu.cn

Authors

Qiong Pan − *State Key Laboratory of Heavy Oil Processing, Petroleum Molecular Engineering Center (PMEC), China University of Petroleum, Beijing 102249, China*

Xiaocun Zhuo − *State Key Laboratory of Heavy Oil Processing, Petroleum Molecular Engineering Center (PMEC), China University of Petroleum, Beijing 102249, China*

Yahe Zhang − *State Key Laboratory of Heavy Oil Processing, Petroleum Molecular Engineering Center (PMEC), China University of Petroleum, Beijing 102249, China*

Complete contact information is available at: https://pubs.acs.org/10.1021/acsomega.9b04411

Notes

The authors declare no competing financial interest.

■ ACKNOWLEDGMENTS

This work was supported by the National Key Research and Development Program of China (2018YFA0605800).

■ REFERENCES

(1) Koch, B. P.; Witt, M.; Engbrodt, R.; Dittmar, T.; Kattner, G. Molecular formulae of marine and terrigenous dissolved organic matter detected by electrospray ionization Fourier transform ion cyclotron resonance mass spectrometry. *Geochim. Cosmochim. Acta* **2005**, *69*, 3299−3308.

(2) Dittmar, T.; Koch, B. P. Thermogenic organic matter dissolved in the abyssal ocean. *Mar. Chem.* **2006**, *102*, 208−217.

(3) Tremblay, L. B.; Dittmar, T.; Marshall, A. G.; Cooper, W. J.; Cooper, W. T. Molecular characterization of dissolved organic matter in a North Brazilian mangrove porewater and mangrove-fringed estuaries by ultrahigh resolution Fourier Transform-Ion Cyclotron Resonance mass spectrometry and excitation/emission spectroscopy. *Mar. Chem.* **2007**, *105*, 15−29.

(4) Amon, R. M. W.; Rinehart, A. J.; Duan, S.; Louchouarn, P.; Prokushkin, A.; Guggenberger, G.; Bauch, D.; Stedmon, C.; Raymond, P. A.; Holmes, R. M.; McClelland, J. W.; Peterson, B. J.; Walker, S. A.; Zhulidov, A. V. Dissolved organic matter sources in large Arctic rivers. *Geochim. Cosmochim. Acta* **2012**, *94*, 217−237.

(5) Flerus, R.; Lechtenfeld, O. J.; Koch, B. P.; McCallister, S. L.; Schmitt-Kopplin, P.; Benner, R.; Kaiser, K.; Kattner, G. A molecular perspective on the ageing of marine dissolved organic matter. *Biogeosciences* **2012**, *9*, 1935−1955.

(6) Melendez-Perez, J. J.; Martínez-Mejía, M. J.; Awan, A. T.; Fadini, P. S.; Mozeto, A. A.; Eberlin, M. N. Characterization and comparison of riverine, lacustrine, marine and estuarine dissolved organic matter by ultra-high resolution and accuracy Fourier transform mass spectrometry. *Org. Geochem.* **2016**, *101*, 99−107.

(7) Fox, P. M.; Nico, P. S.; Tfaily, M. M.; Heckman, K.; Davis, J. A. Characterization of natural organic matter in low-carbon sediments: Extraction and analytical approaches. *Org. Geochem.* **2017**, *114*, 12−22.

(8) Sleighter, R. L.; Hatcher, P. G. Molecular characterization of dissolved organic matter (DOM) along a river to ocean transect of the lower Chesapeake Bay by ultrahigh resolution electrospray ionization Fourier transform ion cyclotron resonance mass spectrometry. *Mar. Chem.* **2008**, *110*, 140−152.

(9) Schmidt, F.; Elvert, M.; Koch, B. P.; Witt, M.; Hinrichs, K.-U. Molecular characterization of dissolved organic matter in pore water of continental shelf sediments. *Geochim. Cosmochim. Acta* **2009**, *73*, 3337−3358.

https://dx.doi.org/10.1021/acsomega.9b04411
ACS Omega 2020, 5, 5372−5379

(10) Koch, B. P.; Kattner, G.; Witt, M.; Passow, U. Molecular insights into the microbial formation of marine dissolved organic matter: recalcitrant or labile? *Biogeosciences* **2014**, *11*, 4173−4190.
(11) Kim, S.; Kramer, R. W.; Hatcher, P. G. Graphical method for analysis of ultrahigh-resolution broadband mass spectra of natural organic matter, the van Krevelen diagram. *Anal. Chem.* **2003**, *75*, 5336−5344.
(12) Chen, M.; Hur, J. Pre-treatments, characteristics, and biogeochemical dynamics of dissolved organic matter in sediments: A review. *Water Res.* **2015**, *79*, 10−25.
(13) Jiang, T.; Kaal, J.; Liang, J.; Zhang, Y.; Wei, S.; Wang, D.; Green, N. W. Composition of dissolved organic matter (DOM) from periodically submerged soils in the Three Gorges Reservoir areas as determined by elemental and optical analysis, infrared spectroscopy, pyrolysis-GC-MS and thermally assisted hydrolysis and methylation. *Sci. Total Environ.* **2017**, *603−604*, 461−471.
(14) Koch, B. P.; Ludwichowski, K.-U.; Kattner, G.; Dittmar, T.; Witt, M. Advanced characterization of marine dissolved organic matter by combining reversed-phase liquid chromatography and FT-ICR-MS. *Mar. Chem.* **2008**, *111*, 233−241.
(15) Hsu, C. S. Mass Resolving Power Requirement for Molecular Formula Determination of Fossil Oils. *Energy Fuels* **2012**, *26*, 1169−1177.
(16) Fievre, A.; Solouki, T.; Marshall, A. G.; Cooper, W. T. High-Resolution Fourier Transform Ion Cyclotron Resonance Mass Spectrometry of Humic and Fulvic Acids by Laser Desorption/Ionization and Electrospray Ionization. *Energy Fuels* **1997**, *11*, 554−560.
(17) Solouki, T.; Freitas, M. A.; Alomary, A. Gas-phase hydrogen/deuterium exchange reactions of fulvic acids: an electrospray ionization Fourier transform ion cyclotron resonance mass spectral study. *Anal. Chem.* **1999**, *71*, 4719−4726.
(18) Brown, T. L.; Rice, J. A. Effect of Experimental Parameters on the ESI FT-ICR Mass Spectrum of Fulvic Acid. *Anal. Chem.* **2000**, *72*, 384−390.
(19) Stenson, A. C.; Marshall, A. G.; Cooper, W. T. Exact masses and chemical formulas of individual Suwannee River fulvic acids from ultrahigh resolution electrospray ionization Fourier transform ion cyclotron resonance mass spectra. *Anal. Chem.* **2003**, *75*, 1275−1284.
(20) Kujawinski, E. B.; Hatcher, P. G.; Freitas, M. A. High-resolution Fourier transform ion cyclotron resonance mass spectrometry of humic and fulvic acids: improvements and comparisons. *Anal. Chem.* **2002**, *74*, 413−419.
(21) Cao, D.; Huang, H.; Hu, M.; Cui, L.; Geng, F.; Rao, Z.; Niu, H.; Cai, Y.; Kang, Y. Comprehensive characterization of natural organic matter by MALDI- and ESI-Fourier transform ion cyclotron resonance mass spectrometry. *Anal. Chim. Acta* **2015**, *866*, 48−58.
(22) Blackburn, J. W. T.; Kew, W.; Graham, M. C.; Uhrín, D. Laser Desorption/Ionization Coupled to FTICR Mass Spectrometry for Studies of Natural Organic Matter. *Anal. Chem.* **2017**, *89*, 4382−4386.
(23) Kim, D.; Lee, J.; Kim, B.; Kim, S. Optimization and Application of Paper-Based Spray Ionization Mass Spectrometry for Analysis of Natural Organic Matter. *Anal. Chem.* **2018**, *90*, 12027−12034.
(24) Willoughby, S. A.; Wozniak, S. A.; Hatcher, G. P. Detailed Source-Specific Molecular Composition of Ambient Aerosol Organic Matter Using Ultrahigh Resolution Mass Spectrometry and 1H NMR. *Atmosphere* **2016**, *7*, 79.
(25) DiDonato, N.; Hatcher, P. G. Alicyclic carboxylic acids in soil humic acid as detected with ultrahigh resolution mass spectrometry and multi-dimensional NMR. *Org. Geochem.* **2017**, *112*, 33−46.
(26) D'Andrilli, J.; Chanton, J. P.; Glaser, P. H.; Cooper, W. T. Characterization of dissolved organic matter in northern peatland soil porewaters by ultra high resolution mass spectrometry. *Org. Geochem.* **2010**, *41*, 791−799.
(27) Heffner, C.; Silwal, I.; Peckenham, J. M.; Solouki, T. Emerging technologies for identification of disinfection byproducts: GC/FT-ICR MS characterization of solvent artifacts. *Environ. Sci. Technol.* **2007**, *41*, 5419−5425.
(28) Zhang, H.; Zhang, Y.; Shi, Q.; Hu, J.; Chu, M.; Yu, J.; Yang, M. Study on Transformation of Natural Organic Matter in Source Water during Chlorination and Its Chlorinated Products using Ultrahigh Resolution Mass Spectrometry. *Environ. Sci. Technol.* **2012**, *46*, 4396−4402.
(29) Gonsior, M.; Schmitt-Kopplin, P.; Stavklint, H.; Richardson, S. D.; Hertkorn, N.; Bastviken, D. Changes in Dissolved Organic Matter during the Treatment Processes of a Drinking Water Plant in Sweden and Formation of Previously Unknown Disinfection Byproducts. *Environ. Sci. Technol.* **2014**, *48*, 12714−12722.
(30) Seidel, M.; Beck, M.; Riedel, T.; Waska, H.; Suryaputra, I. G. N. A.; Schnetger, B.; Niggemann, J.; Simon, M.; Dittmar, T. Biogeochemistry of dissolved organic matter in an anoxic intertidal creek bank. *Geochim. Cosmochim. Acta* **2014**, *140*, 418−434.
(31) Kellerman, A. M.; Dittmar, T.; Kothawala, D. N.; Tranvik, L. J. Chemodiversity of dissolved organic matter in lakes driven by climate and hydrology. *Nat. Commun.* **2014**, *5*, 3804.
(32) Wang, K.; Pang, Y.; He, C.; Li, P.; Xiao, S.; Sun, Y.; Pan, Q.; Zhang, Y.; Shi, Q.; He, D. Optical and molecular signatures of dissolved organic matter in Xiangxi Bay and mainstream of Three Gorges Reservoir, China: Spatial variations and environmental implications. *Sci. Total Environ.* **2019**, *657*, 1274−1284.
(33) Bae, E.; Yeo, I. J.; Jeong, B.; Shin, Y.; Shin, K.-H.; Kim, S. Study of double bond equivalents and the numbers of carbon and oxygen atom distribution of dissolved organic matter with negative-mode FT-ICR MS. *Anal. Chem.* **2011**, *83*, 4193−4199.
(34) Barrow, M. P.; Peru, K. M.; Headley, J. V. An Added Dimension: GC Atmospheric Pressure Chemical Ionization FTICR MS and the Athabasca Oil Sands. *Anal. Chem.* **2014**, *86*, 8281−8288.
(35) Fang, Z.; He, C.; Li, Y.; Chung, K. H.; Xu, C.; Shi, Q. Fractionation and characterization of dissolved organic matter (DOM) in refinery wastewater by revised phase retention and ion-exchange adsorption solid phase extraction followed by ESI FT-ICR MS. *Talanta* **2017**, *162*, 466−473.
(36) Simon, C.; Roth, V.-N.; Dittmar, T.; Gleixner, G. Molecular Signals of Heterogeneous Terrestrial Environments Identified in Dissolved Organic Matter: A Comparative Analysis of Orbitrap and Ion Cyclotron Resonance Mass Spectrometers. *Front. Earth Sci.* **2018**, *6*, 138.
(37) Zhurov, K. O.; Kozhinov, A. N.; Tsybin, Y. O. Evaluation of High-Field Orbitrap Fourier Transform Mass Spectrometer for Petroleomics. *Energy Fuels* **2013**, *27*, 2974−2983.
(38) Hu, Q.; Noll, R. J.; Li, H.; Makarov, A.; Hardman, M.; Graham Cooks, R. The Orbitrap: a new mass spectrometer. *J. Mass Spectrom.* **2005**, *40*, 430−443.
(39) Makarov, A.; Denisov, E.; Kholomeev, A.; Balschun, W.; Lange, O.; Strupat, K.; Horning, S. Performance evaluation of a hybrid linear ion trap/orbitrap mass spectrometer. *Anal. Chem.* **2006**, *78*, 2113−2120.
(40) Makarov, A.; Denisov, E.; Lange, O.; Horning, S. Dynamic range of mass accuracy in LTQ Orbitrap hybrid mass spectrometer. *J. Am. Soc. Mass Spectrom.* **2006**, *17*, 977−982.
(41) Zubarev, R. A.; Makarov, A. Orbitrap mass spectrometry. *Anal. Chem.* **2013**, *85*, 5288−5296.
(42) Cortés-Francisco, N.; Caixach, J. Molecular characterization of dissolved organic matter through a desalination process by high resolution mass spectrometry. *Environ. Sci. Technol.* **2013**, *47*, 9619−9627.
(43) Phungsai, P.; Kurisu, F.; Kasuga, I.; Furumai, H. Molecular characterization of low molecular weight dissolved organic matter in water reclamation processes using Orbitrap mass spectrometry. *Water Res.* **2016**, *100*, 526−536.
(44) Mangal, V.; Stock, N. L.; Guéguen, C. Molecular characterization of phytoplankton dissolved organic matter (DOM) and sulfur components using high resolution Orbitrap mass spectrometry. *Anal. Bioanal. Chem.* **2016**, *408*, 1891−1900.
(45) Patriarca, C.; Bergquist, J.; Sjöberg, P. J. R.; Tranvik, L.; Hawkes, J. A. Online HPLC-ESI-HRMS Method for the Analysis and

https://dx.doi.org/10.1021/acsomega.9b04411
ACS Omega 2020, 5, 5372−5379

Comparison of Different Dissolved Organic Matter Samples. *Environ. Sci. Technol.* **2018**, *52*, 2091−2099.
(46) Soule, M. C. K.; Longnecker, K.; Giovannoni, S. J.; Kujawinski, E. B. Impact of instrument and experiment parameters on reproducibility of ultrahigh resolution ESI FT-ICR mass spectra of natural organic matter. *Org. Geochem.* **2010**, *41*, 725−733.
(47) Sleighter, R. L.; Chen, H.; Wozniak, A. S.; Willoughby, A. S.; Caricasole, P.; Hatcher, P. G. Establishing a Measure of Reproducibility of Ultrahigh-Resolution Mass Spectra for Complex Mixtures of Natural Organic Matter. *Anal. Chem.* **2012**, *84*, 9184−9191.
(48) Leyva, D.; Tose, L. V.; Porter, J.; Wolff, J.; Jaffé, R.; Fernandez-Lima, F. Understanding the structural complexity of dissolved organic matter: isomeric diversity. *Faraday Discuss.* **2019**, *218*, 431−440.
(49) Tose, L. V.; Benigni, P.; Leyva, D.; Sundberg, A.; Ramírez, C. E.; Ridgeway, M. E.; Park, M. A.; Romão, W.; Jaffé, R.; Fernandez-Lima, F. Coupling trapped ion mobility spectrometry to mass spectrometry: trapped ion mobility spectrometry−time-of-flight mass spectrometry versus trapped ion mobility spectrometry−Fourier transform ion cyclotron resonance mass spectrometry. *Rapid Commun. Mass Spectrom.* **2018**, *32*, 1287−1295.
(50) Hawkes, J. A.; Dittmar, T.; Patriarca, C.; Tranvik, L.; Bergquist, J. Evaluation of the Orbitrap Mass Spectrometer for the Molecular Fingerprinting Analysis of Natural Dissolved Organic Matter. *Anal. Chem.* **2016**, *88*, 7698−7704.
(51) He, C.; Jiang, B.; Shi, Q.; Hsu, C. S. Comment on "Laser Desorption/Ionization Coupled to FTICR Mass Spectrometry for Studies of Natural Organic Matter". *Anal. Chem.* **2018**, *90*, 5965−5967.
(52) Miyabayashi, K.; Naito, Y.; Miyake, M.; Tsujimoto, K. Quantitative Capability of Electrospray Ionization Fourier Transform Ion Cyclotron Resonance Mass Spectrometry for a Complex Mixture. *Eur. J. Mass Spectrom.* **2000**, *6*, 251−258.
(53) Zark, M.; Dittmar, T. Universal molecular structures in natural dissolved organic matter. *Nat. Commun.* **2018**, *9*, 3178.
(54) Kim, S.; Rodgers, R. P.; Marshall, A. G. Truly "exact" mass: Elemental composition can be determined uniquely from molecular mass measurement at ∼0.1mDa accuracy for molecules up to ∼500Da. *Int. J. Mass Spectrom.* **2006**, *251*, 260−265.
(55) Schmidt, E. M.; Pudenzi, M. A.; Santos, J. M.; Angolini, C. F. F.; Pereira, R. C. L.; Rocha, Y. S.; Denisov, E.; Damoc, E.; Makarov, A.; Eberlin, M. N. Petroleomics via Orbitrap mass spectrometry with resolving power above 1 000 000 at m/z 200. *RSC Adv.* **2018**, *8*, 6183−6191.
(56) Smith, D. F.; Podgorski, D. C.; Rodgers, R. P.; Blakney, G. T.; Hendrickson, C. L. 21 Tesla FT-ICR Mass Spectrometer for Ultrahigh-Resolution Analysis of Complex Organic Mixtures. *Anal. Chem.* **2018**, *90*, 2041−2047.
(57) Hu, M.; Zhang, L.; He, S.; Xu, C.; Shi, Q. Collision cross section (CCS) measurement by ion cyclotron resonance mass spectrometry with short-time Fourier transform. *Rapid Commun. Mass Spectrom.* **2018**, *32*, 751−761.
(58) Strife, R. J.; Wang, Y.; Kuehl, D. Restricted spectral accuracy analysis to identify the single correct organic compound elemental-composition from Orbitrap accurate mass data lists obtained at very high resolution. *J. Mass Spectrom.* **2018**, *53*, 921−926.
(59) Mitchell, J. M.; Flight, R. M.; Moseley, H. N. B. Small Molecule Isotope Resolved Formula Enumeration: A Methodology for Assigning Isotopologues and Metabolite Formulas in Fourier Transform Mass Spectra. *Anal. Chem.* **2019**, *91*, 8933−8940.
(60) Hertkorn, N.; Frommberger, M.; Witt, M.; Koch, B. P.; Schmitt-Kopplin, P.; Perdue, E. M. Natural Organic Matter and the Event Horizon of Mass Spectrometry. *Anal. Chem.* **2008**, *80*, 8908−8919.
(61) Witt, M.; Fuchser, J.; Koch, B. P. Fragmentation studies of fulvic acids using collision induced dissociation fourier transform ion cyclotron resonance mass spectrometry. *Anal. Chem.* **2009**, *81*, 2688−2694.
(62) Kim, D.; Kim, S.; Son, S.; Jung, M.-J.; Kim, S. Application of Online Liquid Chromatography 7 T FT-ICR Mass Spectrometer Equipped with Quadrupolar Detection for Analysis of Natural Organic Matter. *Anal. Chem.* **2019**, *91*, 7690−7697.
(63) Melendez-Perez, J. J.; Martínez-Mejia, M. J.; Eberlin, M. N. A reformulated aromaticity index equation under consideration for non-aromatic and non-condensed aromatic cyclic carbonyl compounds. *Org. Geochem.* **2016**, *95*, 29−33.
(64) Koch, B. P.; Dittmar, T. From mass to structure: an aromaticity index for high-resolution mass data of natural organic matter. *Rapid Commun. Mass Spectrom.* **2006**, *20*, 926−932.
(65) Li, Y.; Harir, M.; Lucio, M.; Gonsior, M.; Koch, B. P.; Schmitt-Kopplin, P.; Hertkorn, N. Comprehensive structure-selective characterization of dissolved organic matter by reducing molecular complexity and increasing analytical dimensions. *Water Res.* **2016**, *106*, 477−487.
(66) Jiang, B.; Kuang, B. Y.; Liang, Y.; Zhang, J.; Huang, X. H. H.; Xu, C.; Yu, J. Z.; Shi, Q. Molecular composition of urban organic aerosols on clear and hazy days in Beijing: a comparative study using FT-ICR MS. *Environ. Chem.* **2016**, *13*, 888−901.
(67) Herzsprung, P.; Hertkorn, N.; von Tümpling, W.; Harir, M.; Friese, K.; Schmitt-Kopplin, P. Understanding molecular formula assignment of Fourier transform ion cyclotron resonance mass spectrometry data of natural organic matter from a chemical point of view. *Anal. Bioanal. Chem.* **2014**, *406*, 7977−7987.

https://dx.doi.org/10.1021/acsomega.9b04411
ACS Omega 2020, 5, 5372−5379